INFOTEH-JAHORINA Vol. 14, March 2015.

Restoration of defocused digital images

Ratko Ivkovic / Risto Bojovic / Mile Petrovic
Department of Electronic and Computer Engineering
University of Pristina, Faculty of Technical Sciences
Kosovska Mitrovica, Serbia
ratko.ivkovic@pr.ac.rs / risto.bojovic@pr.ac.rs / mile.petrovic@pr.ac.rs

Mirko Milosevic
SP Audio and Video Technologies
The School of Electrical and Computer Engineering
Belgrade, Serbia
mirko.milosevic@viser.edu.rs

Nebojsa Denic
Faculty of information technology
Alfa University
Belgrade, Serbia
nebojsa.denic@alfa.edu.rs

Abstract—**This paper gives the analysis of defocused and blurred images using different algorithms. The restoration was carried out by simulating the real images in the program package MATLAB. The analysis also includes the existence of the real noise in digital images generated during the creation, transmission or processing of the images, which gives particular weight to this paper because it simulates real situations. All used simulations were performed through the frequency and spatial (matrix) domain. To measure the quality of the image we have been using entropy analysis of an image and measure of the level of details for the compression in the discrete cosine transform. The results can be used to improve image quality, but also as a basis for further consideration.**

Keywords-Digital image; Defocusing; Level of Detail (LoD); Entropy

I. INTRODUCTION

Nowadays, according to theoretical and practical point of view, restoration of damaged images is one of the most important and most interesting area of Digital Image Processing (DIP). The restoration of digital images can be considered through several aspects:

- reconstruction of low-resolution images,
- reconstruction of old images,
- reconstruction of defocused images,
- reconstruction of blurred images.

In many situations, it is desirable to get the improved image from a defocused or blurred image. Best examples can be found at images from camera made with wrong focus, or blurred due to shooting in motion or at motion. Partial image restoration is possible with various filters such as Unsharp filter, Wiener filter, Tikhonov filtration, etc. According to applied algorithm some filters do not support whole image restoration. In these cases restoration is only possible for some areas of image - such as edges. Due to these limitations edge restoration is equal to the radius of image blurring. In other words, it is very important that the number of pixels during the reconstruction processes and after them, maintain the same numerical level.

This can be practically demonstrated with the example of one-dimensional images (images with only one channel, such us black and white or grayscale images). If we randomly selected pixels in a row (or column), x_1, x_2, x_3, x_4 from the original image [1], after the blurring process, each pixel value will increase with value of the next pixel value divided by 2:

$$x'_i = \frac{x_i + x_{i-1}}{2} \tag{1}$$

Now pixels' value after the blurring are:

$$x_1 + x_0, x_2 + x_1, x_3 + x_2, x_4 + x_3\,. \tag{2}$$

In this case, after the reconstruction, all 2n-1 pixels are added with initial determined pixel value, and on the other side 2n pixel will be deducted. The equation of reconstructed images becomes:

$$x_1 + x_0, x_2 - x_0, x_3 + x_0, x_4 - x_0 \ldots \tag{3}$$

The result of this process is the image where every pixel is added/subtracted with unknown constant x_0, respectively. The described situation does not take into account the impact of noise accumulation in the image. Depending on the type and origin of the noise reconstruction results can be almost unacceptable.

Central problems in DIP are the optimization and compression. Numerous research papers deal with efficient compression for certain areas of the image, when it is necessary to emphasize particular part of the image. This paper describes the opposite process, the process from blurred and defocused images with the help of inverse function and deconvolutions algorithms applied to images with clearly defined edges.

II. Theoretical Framework

A. Blurring function

Central part of this reconstruction is done by Matlab software package as a standard program for digital signal processing. Based on paper [2], and Fig. 1 graphically was introduced the process of blurring functions Point Spread Function (PSF). This function has a main purpose in the absorption of the side effects in the process of creating an image, as well as the partial elimination of compression errors (different types of noises – Gaussian, salt & pepper, Poisson, etc.).

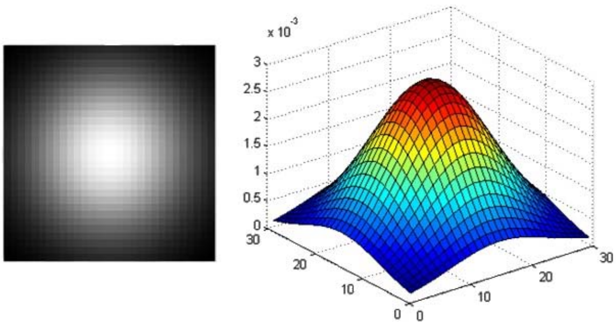

Figure 1. PSF in Gaussian function: fspecial('gaussian', 35, 10)

For that purposes in this paper, inverse function of blur will be used inverse for pulling the useful information from the defocused image. PSF is aimed at “spreading” the desired areas of the image with the help of Gaussian functions. Software implementation shown as:

```
sigma = 2;
X = -10:10;
Gaus = 1/(sqrt(2*pi)*sigma)*exp(-0.5*X.^2/(sigma^2));
```

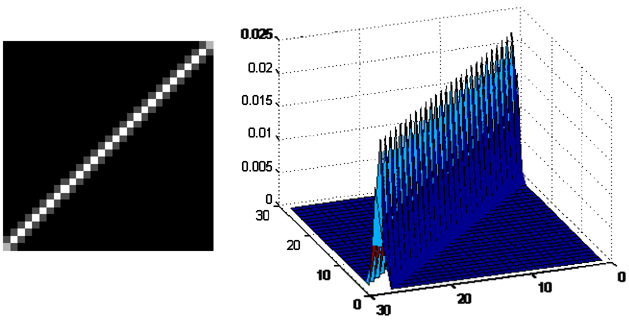

Figure 2. PSF in blur function: fspecial('motion', 35, 50)

Applying one blurring function to another function is called convolution function. The graphic representation of convolution function is presented at Fig. 2. In this way, some image areas under the convolution functions become blurred image areas. Mathematically, if some image *f* (with dimensions *mxn*), *h* blurs function with same dimensions (*mxn*), then applies:

$$g(x,y) = h(x,y) * f(x,y) = \sum_{i=-a}^{a} \sum_{j=-b}^{b} h(i,j)\, f(x+i, y+j)\,, \quad (4)$$

where is:

$$a = \frac{(m-1)}{2}\,,\; b = \frac{(n-1)}{2}\,. \quad (5)$$

These and similar methods represent the core of the image compression. The reason for this is the fact that the large image areas are covered with fewer pixels with characteristic values, thus, the image takes less storage space. The inverse process to convolution function (deconvolution) is very rarely used.

B. Noise

There are many reasons why the damages are occurring in the digital image. The main reasons for damaging an image are thermal vibrations (Brownian motion), the different types of optics, ISO value, types of optical sensors, the value of the magnetic field, temperature, etc. [3]. In the most real situation Gaussian noise is the central problem. There are no rules for Gaussian noise dispersion on the image; thus, from channels (R, G, B) we have three completely different functions of noise distribution. If this is taken into consideration, than the only way to describe noise is through random distribution function. This fact represents the main problem for modern algorithms dealing with the noise elimination. All these facts are taken as a basis during the analysis required for this research.

C. Convolution theory

This research uses only convolution methods which takes into account the impurities of the image. Equation (6) give us large sum $h(x,y)$ and $f(x,y)$ due to high complicity of calculations for a computer. In that case Fourier transform [4] was used, in which convolution operation in the spatial domain is equivalent to multiplication in the frequency domain (multiplied element-by-element). The operation opposite to the convolution is the equivalent to splitting in the frequency domain, and is expressed as follows:

$$h(x,y) * f(x,y) \Leftrightarrow H(u,v)F(u,v)\,. \quad (6)$$

Where $H(u, v)$ and $F(u, v)$ represents the Fourier functions for $h(x, y)$ and $f(x, y)$. Thus, the process of blurring can be written in the frequency domain as:

$$G(u,v) = H(u,v)F(u,v) + N(u,v)\,. \quad (7)$$

where $N(u, v)$ represents a function of the added noise. However, the specific character of these functions can be observed during the implementation of the Tikhonov regularization.

D. The inverse filter

If the equation (7) divided by $H(u, v)$, we get the following equation from the original image [5]:

$$\hat{F}(u,v) = F(u,v) + \frac{N(u,v)}{H(u,v)}\,. \quad (8)$$

On the other hand, the function of the inverse filter $\hat{F}(u,v)$ can be treated as:

$$\hat{F}(u,v) = \frac{G(u,v)}{H(u,v)} \tag{9}$$

This inverse filter is the core algorithms such as Lucy-Richardson and Blind deconvolution.

III. Methodology

This paper used the image of a square resolution (512x512 pixels), with 96 dots per inch and 24 bit color depth (8 per channel). Image format is RGB. All applied process is performed separately for each channel. Due to their comprehensiveness all shown results are for two analysed images. Two blurry and defocused images are shown in Fig. 3.

According all above defocused image can be described by the function:

$$g(x,y) = h(x,y) * f(x,y) + n(x,y) . \tag{10}$$

where is:

- $f(x, y)$ – original image,
- $h(x, y)$ – blur function,
- $n(x, y)$ – function of the added noise,
- $g(x, y)$ – reconstructed image.

The main task of blurred and defocused image restoration is to find the value of function $f'(x,y)$ of approximate value of image that is not blurred. Some of the examples require finding the values of the images that are not blurred, as shown in this analysis. Due to the fact that original defocused image does not exists, analysis of calculated results was done by visual perception of quality and parameters for grading the quality of Entropy and Level of Details.

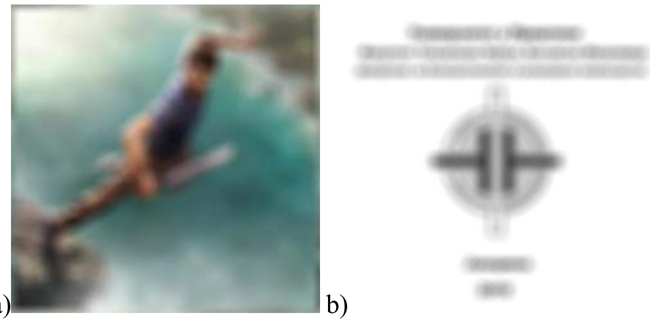

a) b)

Figure 3. Original images (defocused and blured images), a) Far Cry, b) FTN

The function $h(x, y)$ gives the significance for the entire process, because from the blurred images with visually unrecognizable objects provides a visually identifiable objects for further analysis, and the useful image as well. After the adding $h(x, y)$ to the functions of added noise $n(x, y)$ image is ready for analysis. All images used in this analysis are in TIFF image format. This kind of format keeps the image without compression; this helps eliminating the side effects of the compression, and the influence of compression on the final result. Taking into account all the facts, analysis was performed according to the function of the random distribution for added noise per each channel individually. The main reason for that is possibility to control function via the noise dispersion parameter. After this process, some pixels become “wider” thanks to blurred function or PSF. The size of a blur function is smaller than the function on which it has an influence. The reason for this we can find in pixel value which consists of the sum/difference of two neighbouring pixels. Because of that all the obtained images are subject to impact of deconvolution algorithm and inverse filter.

IV. Results and Analysis

The approach for reconstruction and filter selection for noise elimination depends on applied formula for frequency or spatial domain. At first step analysis was done through filter for noise elimination. With this step we eliminated the possibility of noise accumulation for the next step. The filter that gives the best results in this area of DIP, especially for Gaussian noise is the Wiener filter [6]. The analysis of this filter is performed in the frequency domain based on the equation (11):

$$\hat{F}(u,v) = \left(\frac{1}{H(u,v)} \frac{|H(u,v)|^2}{|H(u,v)|^2 + \dfrac{S_\eta(u,v)}{S_f(u,v)}} \right) G(u,v) . \tag{11}$$

After the analysis of defocused images (shown on Fig. 3) by using Wiener filter, the reconstructed images are obtained (Fig. 4). Numerical result of entropy and the level of detail presented in the Table 1.

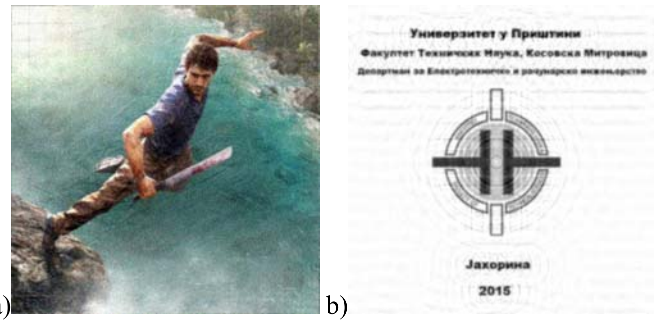

a) b)

Figure 4. Reconstruction by the Wiener filter

Another defocusing reconstruction model “Constrained Least Squares Filtering” is also known as “Tikhonov filtration” or “Tikhonov regularization” [7] in DIP literature. It is based on the spatial (matrix) analysis, and reconstruction is performed for all three channels individually according to the following equation:

$$\hat{F}(u,v) = \left(\frac{H^*(u,v)^2}{|H(u,v)|^2 + y\,|P(u,v)|^2} \right) G(u,v) . \tag{12}$$

Where the y is the regulation parameter, and the P (u, v) is Fourier function for the Laplace operator in the 3x3 matrix.

Based on all previous research papers in the field of DIP, on the spatial domain, Laplace operator gives enviable good results in the process of elimination of accumulation noises, because of that it represents the best choice for this purpose. Filtering matrix 3x3 represents matrix with lowest order and the smallest degree of an error - that was the main reason for using it in the analysis. Reconstruction results after the process with Tikhonov regularization are shown at Fig. 5.

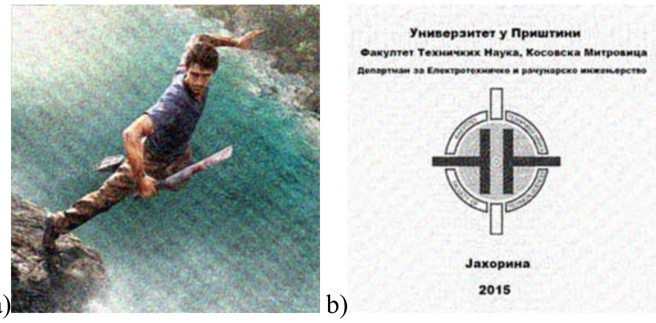

a) b)

Figure 5. Tikhonov regularization

The third reconstruction is performed with the help of Lucy-Richardson algorithm (shown in Fig. 6), based on the implementation of nonlinear function [8]. Method of maximum value in the frequency domain is used for elimination of the Poisson noise. It is very important to say that Fourier transformation is not used in this algorithm. Realization model is performed according to following equation:

$$\hat{f}_{k+1}(u,v) = \hat{f}_k(u,v)\left[h(-u,-v) * \frac{g(u,v)}{h(u,v) * \hat{f}_k(u,v)}\right]. \quad (13)$$

The symbol "*" in the equation above expresses the convolution function.

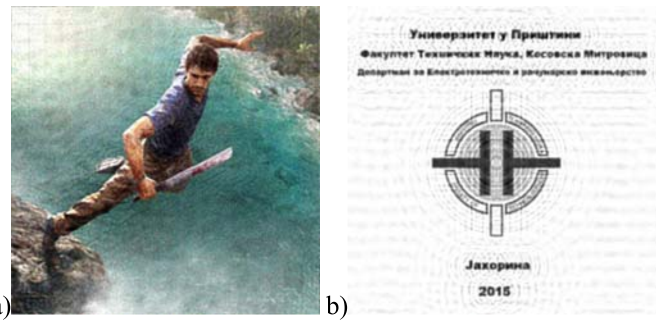

a) b)

Figure 6. Lucy-Richardson filter

The next image reconstruction was performed with the help of blind deconvolution methods [9]. This type of reconstruction uses PSF as a core for this algorithm, because of that blind deconvolution is different from others algorithms [10]. According to all above, the quality of the output image depends on PSF definition. Different set of tools for PSF should be repeated until the output image does not have desirable quality. Deconvolution function returns the reconstructed PSF function in matrix form, as shown in Figure 7. Similar as Lucy-Richardson algorithm, blind deconvolutions gives high quality results in the reconstructed image with Poisson noise.

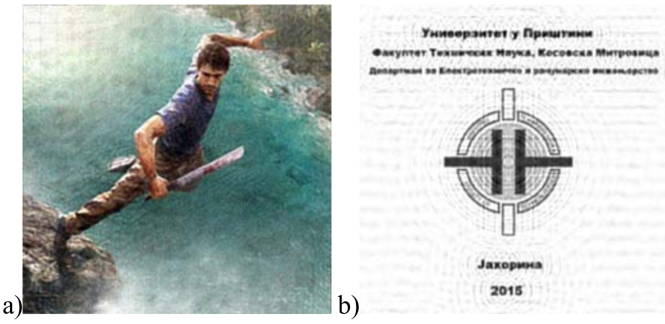

a) b)

Figure 7. Blind deconvolution

$$|\hat{K}_\omega|^2 = max\left(0, \frac{|Y_\omega|^2 - \eta^2}{{\sigma_\omega}^2}\right) \quad (14)$$

In all equations, u and v represent the position of the observed pixel in the image. Also, it is important to say, that the each equation, deals with all three channels separately according to following equation:

```
I = im2double(imread('Far Cry.tiff'));
[u,v,j]=size(I);
```

The entire algorithm is separately calculated for j = 1 (R channel), j = 2 (G channel) and j = 3 (B channel).

Increasing in LoD value is expected for all processed images. The values of the LOD for Discrete Cosine Transform (DCT) can be viewed through the prism of increasing the degree of pixel values variation in the image. This degree of variation can be presented through increasing the level of noise in the images, or in another way through increasing variation real ("desirable") pixels value. Specifically, this shows that defocused images do not have harsh crossings of pixel values. The best proof for assumption like this is the lowest value level for LoD for DCT. According to all above, Tikhonov regularization gives significantly better result over the observed images in comparison to other algorithms. All obtained results are not sufficiently reliable for determination of the image quality, because of that it is necessary to calculate another parameter for better understanding of the image quality. Entropy as a potential measure of image quality gives a significant contribution to assessment of an image as a single signal.

TABLE I. VALUE OF LOD FOR ORIGINAL AND RECONSTRUCTED IMAGES

LoD (DCT)	**Far Cry**	**FTN**
Blurred	0.2673	0.146
Wiener filter	1.8683	0.5452
Tikhonov regularization	1.4075	1.1497
Lucy-Richardson filter	1.1336	0.7643
Blind deconvolution	1.1367	0.7678

Table 1. represents the value of LoD and entropy for the original images and all obtained images. According to all numerical results from Table it can be concluded that in all

tested algorithms is evident drastic increase in the LoD. The degree of LoD increasing going from 4x for the Wiener filter to 7x for Tikhonov regularization. According to all above Tikhonov regularization gives high quality results in comparison to all other algorithms.

Based on Entropy as a measure of the image potential, the Tikhonov regularization algorithm gives the best results. All processed images "have" higher entropy level after the reconstruction. Based on these facts, conclusion is that all the resulting images are better for further processing, if necessary.

TABLE II. LEVEL OF ENTROPY FOR ORIGINAL AND RECONSTRUCTED IMAGES

Entropija [bit]	Far Cry	FTN
Blurred	7.5869	3.8646
Wiener filter	7.7518	4.4411
Tikhonov regularization	7.801	4.5834
Lucy-Richardson filter	7.7595	4.5754
Blind deconvolution	7.7593	4.5732

Table 2 shows the results for entropy of original images and for all images after reconstructions. Numerical data shows that all images kept almost identical value of entropy after the reconstructions. This is good information, because if the visual quality is not at the desirable level for the user it can be subjected for some other algorithms to achieve better quality.

V. CONCLUSION

This paper gives analyses of different types of algorithms used for processing of defocused and blurred images with different levels of details. The analysis was done in a frequency and spatial domain and filters of different kind was used to eliminate the accumulation of noise. An analysis included the existence of the real noise, which occurs during the creation, transmission or the treatment of the image. From the obtained results, visual and numeric one, it can be concluded that the analyses done in spatial domain gives better results than the analyses done in frequency domain. The thesis that the image should be observed through the dimension of pixel as the basic unit of digital image goes in favour to previous conclusion.

Complete analyses of Entropy showed that the best results in reconstruction of defocused images were obtained using the Tikhon's regularization algorithm. It was observed that all analysed images reflected high level of entropy after the treatment. On the other side, images with low level of potential were increasing 3.5 times, which is a positive feature. From the obtained results for the parameter LoD (DCT) it can be conclude that the images with non-adequate visual quality, Tikhonov's regularization algorithm is the most suitable for reconstruction.

Making a linkage of the obtained results and works such as [11] and combinations with different algorithms it is possible to extract useful information from the totally unusable images. Thereby, devices that perform conversion of light into electrical signals (cameras) gain a lot greater possibilities.

ACKNOWLEDGMENT

This work was done within the research project of the Ministry of Science and Technological Development of Serbia TR35026 and III47016.

REFERENCES

[1] R. Raich, A. Arbor, "Sparse Image Reconstruction for Partially known Blur Functions", 2006 IEEE International Conference on Image Processing, pp. 637-640, 8-11 Oct. 2006.

[2] S. Xu, L. Zeng, Z. Z. Li, C. D. Tian, "A pilot measurement of head-related transfer function blur in spatial localization", IEEE International Conference on Industrial Engineering and Engineering Management, pp. 467-471, 2-4 Dec. 2007.

[3] D. Middleton, "Non-Gaussian noise models in signal processing for telecommunications: new methods an results for class A and class B noise models," IEEE Transactions on Information Theory, vol/ 45, no. 4, pp. 1129-1149, May 1999.

[4] B. Hunt, "A matrix theory proof of the discrete convolution theorem," IEEE Transactions on Audio and Electroacoustics, vol. 19, no. 4, pp. 285-288, 29. Jan. 2003.

[5] M. A. Sapia, M. D. Fox, L. M. Loew, J. C. Schaff, "Ultrasound image deconvolution using adaptive inverse filtering," 12th IEEE Symposium on Computer-Based Medical Systems, pp. 248-253, 18-20 Jun 1999.

[6] J.-C. Yoo, C. W. "Ahn, Image restoration by blind-Wiener filter," Image Processing, IET, vol. 8, no. 12, pp. 815-823, 1 Dec. 2014.

[7] C. Wu, J. He, X. Zou, "A Genetic Algorithm approach for selecting Tikhonov regularization parameter," IEEE Congress on Evolutionary Computation, 2008. CEC 2008. (IEEE World Congress on Computational Intelligence), pp. 3980-3983, 1-6 Jun. 2008.

[8] J. Wei, "Image restoration in neutron radiography using complex-wavelet denoising and lucy-richardson deconvolution," 8th International Conference on Signal Processing, vol. 2, 16-20 Nov. 2006.

[9] A. Levin, Y. Weiss, F. Durand, W. T. Freeman, "Understanding and evaluating blind deconvolution algorithms," IEEE Conference on Computer Vision and Pattern Recognition, 2009. CVPR 2009, pp. 1964-1971, 20-25 Jun. 2009.

[10] R. Ivkovic, I. Milosevic, B. Gara, S. Minic, V. Dakovic, "Algoritam za detekciju ivica slike sa postfiltrom," XIII medunarodni naucno-strucni simpozijum INFOTEH 2014, Jahorina, Bosna i Hercegovina, vol. 13, pp. 652-656, 19-21 Mart 2014.

[11] R. Ivkovic, I. Milosevic, B. Gara, S. Minic, D. Miljkovic, "Rekonstrukcija slika vidljivog spektra snimljenih sa malim procentom osvetljenja," XIII međunarodni naučno-stručni simpozijum INFOTEH 2014, Jahorina, Bosna i Hercegovina, vol. 13, pp. 648-651, 19-21 Mar. 2014.

RESTORATION OF DEFOCUSED DIGITAL IMAGES

Ratko Ivkovic, Risto Bojovic, Mile Petrovic, Mirko Milosevic, Nebojsa Denic